Are ancient dwarf satellites the building blocks of the Galactic halo?

E. Spitoni,[1]★ F. Vincenzo,[1,2] F. Matteucci[1,2,3] and D. Romano[4]

[1]*Dipartimento di Fisica, Sezione di Astronomia, Università di Trieste, via G.B. Tiepolo 11, I-34131 Trieste, Italy*
[2]*INAF Osservatorio Astronomico di Trieste, via G.B. Tiepolo 11, I-34131 Trieste, Italy*
[3]*INFN Sezione di Trieste, via Valerio 2, I-34134 Trieste, Italy*
[4]*INAF Osservatorio Astronomico di Bologna, via Ranzani 1, I-40127 Bologna, Italy*

ABSTRACT

According to the current cosmological cold dark matter paradigm, the Galactic halo could have been the result of the assemblage of smaller structures. Here we explore the hypothesis that the classical and ultra-faint dwarf spheroidal satellites of the Milky Way have been the building blocks of the Galactic halo by comparing their [α/Fe] and [Ba/Fe] versus [Fe/H] patterns with the ones observed in Galactic halo stars. The α elements deviate substantially from the observed abundances in the Galactic halo stars for [Fe/H] values larger than −2 dex, while they overlap for lower metallicities. On the other hand, for the [Ba/Fe] ratio, the discrepancy is extended at all [Fe/H] values, suggesting that the majority of stars in the halo are likely to have been formed *in situ*. Therefore, we suggest that [Ba/Fe] ratios are a better diagnostic than [α/Fe] ratios. Moreover, for the first time we consider the effects of an enriched infall of gas with the same chemical abundances as the matter ejected and/or stripped from dwarf satellites of the Milky Way on the chemical evolution of the Galactic halo. We find that the resulting chemical abundances of the halo stars depend on the assumed infall time-scale, and the presence of a threshold in the gas for star formation. In particular, in models with an infall time-scale for the halo around 0.8 Gyr coupled with a threshold in the surface gas density for the star formation (4 $M_\odot$ pc^{-2}), and the enriched infall from dwarf spheroidal satellites, the first halo stars formed show [Fe/H]>−2.4 dex. In this case, to explain [α/Fe] data for stars with [Fe/H]<−2.4 dex, we need stars formed in dSph systems.

Key words: ISM: abundances – Galaxy: abundances – Galaxy: evolution – Galaxy: halo.

1 INTRODUCTION

The formation and evolution of the Milky Way (MW) halo has been the subject of several investigations in the past years, and a great deal of observational work has been done in order to obtain more and more precise abundance determinations in stars in the Galaxy and Local Group galaxies. We recall here a number of ongoing and planned spectroscopic MW survey, such as RAVE (Steinmetz et al. 2006), SEGUE (Yanny et al. 2009), APOGEE (Majewski et al. 2010), HERMES (Freeman 2010), *Gaia*-ESO (Gilmore et al. 2012).

A crucial information regarding the dominant mechanisms responsible for the formation of the MW halo is encoded in the chemical and kinematical properties of its member stars. In particular, the study of the MW stellar halo provides several clues about the earliest phases of the Galaxy evolution, since the halo is the easiest place where to find the most metal-poor and oldest stars currently

known in the Universe although very old stars could be found also in the bulge of the MW (White & Springel 2000).

The current cosmological Λ cold dark matter (ΛCDM) paradigm envisages the assemblage of large structures in the Universe as starting from the coalescence of smaller ones, via cooling and condensation of gas in always larger dark matter (DM) haloes (Press & Schechter 1974; White & Rees 1978; Springel, Frenk & White 2006). According to the ΛCDM model, a MW-like galaxy must have formed by the coalescence of a large number of smaller systems which, even today, might be still in the process of being accreted. In particular, dwarf spheroidal galaxies (dSphs) were proposed in the past as the best candidate small progenitor systems, which merged through cosmic time to eventually form the stellar halo component of the Galaxy (e.g. Grebel 2005). The MW dSph satellites have been soon recognized among the faintest and most DM-dominated stellar systems ever observed in the Universe, before the discovery of ultra-faint dwarf galaxies. Nevertheless, the role played by dSphs in shaping the halo of the MW still remains controversial. Major issues are the still relatively small number of discovered Galaxy satellites (the so-called missing satellite problem; e.g. Klypin et al. 1999; Moore et al. 1999; Bullock 2010) and the different

★ E-mail: spitoni@oats.inaf.it

chemical abundance patterns in halo and dSph stars (Shetrone, Côté & Sargent 2001; Venn et al. 2004; Vincenzo et al. 2014).

In order to test the capability of the hierarchical galaxy formation scenario to explain the MW halo metallicity distribution function (MDF), Prantzos (2008) presented the results of an approximated analytical model, where the Galaxy stellar halo was assumed to assemble by means of successive merger events of small sub-haloes with similar physical properties as current dSphs. Although the treatment of the interstellar medium (ISM) chemical evolution was very simple, Prantzos (2008) claimed to reproduce the Galaxy halo MDF, since his results rely on the stellar mass distribution function of the merging sub-halo population, which the current hierarchical galaxy formation paradigm can predict with very high accuracy. Nevertheless, Prantzos (2008) did not discuss any implication on the [α/Fe] versus [Fe/H] abundance pattern, which is one of the main issues which hierarchical picture has to deal with, since the abundance patterns of surviving Local Group galaxies do not match those of the stars in the stellar halo.

It is worth reminding that Unavane, Wyse & Gilmore (1996) and Jofré & Weiss (2011) used the age distributions of stars in the halo and dSphs to test the origin of halo stars.

Interestingly, by making use of a chemical evolution model within a cosmological framework, Font et al. (2006) found that the discrepancy in the [α/Fe] ratios can be solved if the majority of the MW halo formed by accreting sub-haloes with mass in the range 10^5–10^8 M$_\odot$, which had been disrupted very early ($>$8–9 Gyr ago).

On the other hand, Fiorentino et al. (2015) using RR Lyrae stars as tracers of the Galactic halo ancient stellar component, showed that dSphs do not appear to be the major building-blocks of the halo. Leading physical arguments suggest an extreme upper limit of 50 per cent to their contribution.

In recent years, Willman et al. (2005) and Belokurov et al. (2006a,b, 2007) using the Sloan Digital Sky Survey (York et al. 2000) were able to discover an entirely new population of hitherto unknown stellar systems: the so-called ultra-faint dwarf spheroidal galaxies (UfDs), which are characterized by extremely low luminosities, high DM content, and very old and iron-poor stellar populations (Belokurov et al. 2006b; Norris et al. 2008, 2010; Brown et al. 2012). Furthermore, UfD systems are observed to be completely gas-free at the present time. The number of UfDs has increased constantly in the last decade and completeness estimates suggest that many more of these faint satellites are still to be discovered in the Local Group (Tollerud et al. 2008). This fact might place them as the survived building blocks of the Galaxy stellar halo, dramatically lacking in the past.

The main aims of this work can be summarized as follows.

(i) We test the hypothesis that dSph and UfD galaxies have been the building blocks of the Galactic halo, by assuming that the halo formed by accretion of stars belonging to these galaxies.

(ii) We explore the scenario, in which the Galactic halo formed by accretion of chemically enriched gas originating from dSph and UfD galaxies.

In Spitoni (2015), using the formalism described by Matteucci (2001), Recchi et al. (2008), and Spitoni et al. (2010) it was shown, for the first time, an analytical solution for the evolution of the metallicity of a galaxy in presence of 'environment' effects. In this work, a galaxy suffers, during its evolution, the infall of enriched gas from another evolving galactic system, with this gas having chemical abundances variable in time.

In this work, we extend the results of Spitoni (2015) to detailed chemical evolution models in which the Instantaneous Recycling

Approximation is relaxed, for the particular case of the chemical enrichment of the Galactic halo surrounded by dSph and UfD galaxies.

The paper is organized as follows: in Section 2, we present our chemical evolution models for the Galaxy, dSph and UfD galaxies, in Section 3, we describe the way in which we implement the enriched gas infall on the chemical evolution of the Galactic halo. The results are presented in Section 4. Finally, our conclusions are summarized in Section 5.

2 THE CHEMICAL EVOLUTION MODELS

In this work, for the first time, we present a chemical evolution model where we assume that the Galactic halo is formed by accretion of enriched gas with chemical abundances identical to those of gas outflowing/stripped from dSph, and UfD galaxies. In this section, we will give some details related to the reference chemical evolution models considered in this paper for the MW, dSph, and UfD galaxies.

For the star formation rate (SFR), all the MW models adopt the following Kennicutt (1998) like law:

$$\psi(t) \propto \nu \sigma_g^k, \tag{1}$$

where ν is the star formation efficiency (SFE), σ_g is the surface gas density, and k is the gas surface exponent, with an exponent $k = 1.5$. On the other hand, the SFRs of dSph and UfD galaxies are considered proportional to the volume gas density ρ_g with an exponent $k = 1$:

$$\psi(t) \propto \nu \rho_g^k. \tag{2}$$

In Romano et al. (2015), it is recalled that originally Kennicutt (1998) law refers to surface densities. They show that for star-forming regions with roughly constant scaleheights, the surface densities can be turned into volume densities. Moreover, using the fact that the Kennicutt law indicates that the SFR is controlled by the self-gravity of the gas, it is possible to show the equivalence between $k = 1.5$ in equation (1) and $k = 1$ in equation (2).

2.1 The Milky Way

We will consider the following two reference chemical evolution models for the MW galaxy.

(i) The classical two-infall model (2IM) presented by Brusadin et al. (2013), which is an updated version of the 2IM of Chiappini, Matteucci & Gratton (1997). The Galaxy is assumed to have formed by means of two main infall episodes: the first formed the halo and the thick disc, the second the thin disc. The accretion law of a certain element i at the time t and Galactocentric distance r is defined as

$$A(r, t, i) = X_{A_i} \left(a(r)e^{-t/\tau_H(r)} + b(r)e^{-(t-t_{max})/\tau_D(r)} \right). \tag{3}$$

The quantity $X_{A_i} = \sigma_i(t)/\sigma_{gas}(t)$ is the abundance by mass of the element i in the infalling material, while $t_{max} = 1$ Gyr is the time for the maximum infall on the thin disc, $\tau_H = 0.8$ Gyr is the time-scale for the formation of the halo and thick disc and $\tau_D(r)$ is the time-scale for the formation of the thin disc and is a function of the galactocentric distance (inside-out formation; Matteucci & François 1989; Chiappini, Matteucci & Romano 2001). In the 2IM model, the abundances X_{A_i} show primordial gas compositions and are constant in time.

Finally, the coefficients $a(r)$ and $b(r)$ are obtained by imposing a fit to the observed current total surface mass density in the different

Table 1. Parameters of the chemical evolution models for the Milky Way (Brusadin, Matteucci & Romano 2013) in the solar neighbourhood.

Models	Infall type	τ_H (Gyr)	τ_D (Gyr)	Threshold $(M_\odot pc^{-2})$	k	ν (Gyr^{-1})	IMF	ω (Gyr^{-1})
				The Milky Way: the solar neighbourhood model parameters				
2IM	2 infall	0.8	7	4 (halo-thick disc) 7 (thin disc)	1.5	2 (halo-thick disc) 1 (thin disc)	Scalo (1986)	–
2IMW	2 infall	0.2	7	4 (halo-thick disc) 7 (thin disc)	1.5	2 (halo-thick disc) 1 (thin disc)	Scalo (1986)	14

considered Galactic components as a function of the Galactocentric distance; for instance, for the thin disc:

$$\sigma(r) = \sigma_0 e^{-r/r_D}, \tag{4}$$

where $\sigma_0 = 531\,M_\odot\,pc^{-2}$ is the central total surface mass density and $r_D = 3.5$ kpc is the scalelength. The halo surface mass density at solar position is quite uncertain and we assume it to be $17\,M_\odot\,pc^{-2}$ in the solar neighbourhood. In fact, the total surface mass density in the solar vicinity is $\sim71\,M_\odot\,pc^{-2}$ (Kuijken & Gilmore 1991) with $\sim54\,M_\odot\,pc^{-2}$ corresponding to the disc surface mass density.

(ii) The 2IM plus outflow of Brusadin et al. (2013; in this work, we will indicate it as the 2IMW model). In this model, a gas outflow occuring during the halo phase with a rate proportional to the SFR through a free parameter is considered. Following Hartwick (1976), the outflow rate is defined as

$$\frac{d\sigma_w}{dt} = -\omega\psi(t), \tag{5}$$

where ω is the outflow efficiency.

In Table 1, the principal characteristics of the two chemical evolution models for the MW are summarized: in the second column, the infall type is indicated, in the third, and in the fourth columns, the time-scale τ_H of halo formation and the time-scale τ_D of the thin disc formation, are drawn. The adopted threshold in the surface gas density for the star formation (SF) is reported in columns 5. In column 6, the exponent of the Schmidt (1959) law is shown, in columns 7 and 8, we report the SF efficiency and the initial mass function (IMF), respectively. Finally, in the last column, the presence of the wind is indicated in term of the efficiency ω.

In this work, we only focus on the study of the halo phase, investigating the effects of the pre-enriched infall of gas assuming chemical abundances taken from the outflowing/stripped gas from dSph and UfD galaxies. We assume that the halo phase spans the range of [Fe/H] up to -1 dex. It is important to underline that in our model we do not modify the gas infall laws of the Brusadin et al. (2013) model, and the way in which the Galaxy is built up remains the same. Here, we only consider a time dependent enriched infall, i.e. $X_{A_i}(t)$, with the same chemical abundances of the outflowing gas from dSph and UfD galaxies.

Concerning the observational data for the α elements and Fe, as done in Micali, Matteucci & Romano (2013), we employ only data in which NLTE corrections are considered. In particular, the data we use for Galactic halo stars are from Gratton et al. (2003), Cayrel et al. (2004), Akerman et al. (2004), Mashonkina, Korn & Przybilla (2007) and Shi et al. (2009). For Ba, we use the data of Frebel (2010), as selected and binned by Cescutti et al. (2013).

2.2 The dSph and UfD galaxies

To model the chemical evolution of dSph and UfD galaxies, we refer to the work of Vincenzo et al. (2014). In Tables 2 and 3, the main parameters of generic models for 'classical' dSph and UfD galaxies are reported, respectively. The SFE ν, the exponent k of the Kennicutt (1998) law, and the wind efficiency ω are drawn in column one, two and three, respectively. In the other columns are reported: the infall time-scale (column 4), the period of major SF activity in which the 99 per cent of stars are formed (column 5); total infall gas mass (column 6); mass of the DM halo (column 7); effective radius of the luminous (baryonic) matter (column 8); ratio between the core radius of the DM halo and the effective radius of the luminous matter (column 9); in column 10, the adopted IMF is indicated. In column 11, the time of the onset of the galactic wind is reported. In the last column, we show the [Fe/H] abundance of the peak of the predicted G-dwarf metallicity distribution. We assume that UfD objects are characterized by a very small SFE (0.01 Gyr^{-1}) and by an extremely short time-scale of formation (0.001 Gyr). Hence, UfD objects started to form stars as most of their infall mass, $M_{inf} = 10^5\,M_\odot$, was accumulated in their DM potential well ($\tau_{inf} = 0.001$ Gyr) and the SFE is very low ($\nu = 0.01$ Gyr^{-1}). Our chemical evolution model for a typical dSph galaxy assumes an infall mass $M_{inf} = 10^7\,M_\odot$, an infall time-scale $\tau_{inf} = 0.5$ Gyr, and an SFE $\nu = 0.1$ Gyr^{-1}. Although the star formation history (SFH) is assumed to be extended over the entire galaxy lifetime both for the dSph and the UfD galaxy, it is strongly concentrated in the earliest stages of the galaxy evolution; in fact, as most of the infall mass has been accumulated and the galactic wind has started, the intensity of the SFR becomes negligible. We acknowledge that this kind of SFR history is not representative in particular of the more luminous dSph galaxies (e.g. Weisz, Johnson & Conroy 2014). We point out that, in the modelling of the dSphs and UfDs, we did not consider any threshold in the gas density for SF, as in Vincenzo et al. (2014).

The time at which the galactic winds start in dSph and UfD models. For the dSph, the galactic wind occurs at 0.013 Gyr after the galactic formation, whereas for UfDs at 0.088 Gyr.

As expected, the UfD galaxies develop a wind at later times because of the smaller adopted SFE. Moreover, because of the shorter formation time-scale, the UfDs show the G-dwarf metallicity peak at lower [Fe/H] values compared to dSph galaxies.

2.3 Nucleosynthesis prescriptions

In this work, we adopt the nucleosynthesis prescriptions of Romano et al. (2010, model 15), who provide a compilation of stellar yields able to reproduce several chemical abundance patterns in the solar neighbourhood. In particular, they assume the following sets of stellar yields.

(i) For low- and intermediate-mass stars (0.8–8 M$_\odot$), they include the metallicity-dependent stellar yields of Karakas (2010). For Type Ia supernova (SNe Ia), the adopted nucleosynthesis prescriptions are from Iwamoto et al. (1999).

Table 2. Parameters of the chemical evolution model for a general dSph galaxy.

				dSphs: parameters of the model							
ν (Gyr^{-1})	k	ω	τ_{inf} (Gyr)	SFH (99 per cent of stars) (Gyr)	M_{inf} (M$_\odot$)	M_{DM} (M$_\odot$)	r_L (pc)	$S = \frac{r_L}{r_{DM}}$	IMF	t_{gw} (Gyr)	[Fe/H]$_{peak}$ [dex]
0.1	1	10	0.5	0–2.43	10^7	$3.4 \cdot 10^8$	260	0.52	Salpeter (1955)	0.013	−2.10

Table 3. Parameters of the chemical evolution model for a general dSph galaxy.

				UfDs: parameters of the model							
ν (Gyr^{-1})	k	ω	τ_{inf} (Gyr)	SFH (99 per cent of stars) (Gyr)	M_{inf} (M$_\odot$)	M_{DM} (M$_\odot$)	r_L (pc)	$S = \frac{r_L}{r_{DM}}$	IMF	t_{gw} (Gyr)	[Fe/H]$_{peak}$ (dex)
0.01	1	10	0.001	0–0.49	10^5	10^6	35	0.1	Salpeter (1955)	0.088	−3.30

(ii) For massive stars ($M > 8_\odot$), which are the progenitors of either SNe II or HNe, depending on the explosion energy, they assume the metallicity-dependent He, C, N and O stellar yields, as computed with the Geneva stellar evolutionary code, which takes into account the combined effect of mass-loss and rotation (Meynet & Maeder 2002; Hirschi 2005; Hirschi 2007; Ekström et al. 2008); for all the elements heavier than oxygen, they assume the up-to-date stellar evolution calculations by Kobayashi et al. (2006).

For barium, we assume the stellar yields of Cescutti et al. (2006, model 1, table 4). In particular, Cescutti et al. (2006) includes the metallicity-dependent stellar yields of Ba as computed by Busso et al. (2001), in which barium is produced by low-mass AGB stars, with mass in the range $1.0 \leq M \leq 3.0$ M$_\odot$, as an *s*-process neutron capture element. A second channel for the Ba-production was included by Cescutti et al. (2006), by assuming that massive stars in their final explosive stage are capable of synthesizing Ba as a primary *r*-process element. Such *r*-process Ba producers have mass in the range $12 \leq M \leq 30$ M$_\odot$.

We remark on the fact that the contribution to barium from massive stars was empirically computed by Cescutti et al. (2006), by matching the [Ba/Fe] versus [Fe/H] abundance pattern as observed in the Galactic halo stars. They assumed for massive stars the iron stellar yields of Woosley & Weaver (1995), as corrected by François et al. (2004).

3 THE ENRICHED INFALL OF GAS

The novelty of this work is to take into account in a self-consistent way time-dependent abundances, i.e. $X_{A_i} = X_{A_i}(t)$ instead of $X_{A_i} = $ constant in equation (3) for the accreting gas in the halo phase, with the values of $X_{A_i}(t)$ corresponding to the chemical abundances of the material ejected from dSph and UfD galaxies by means of their galactic winds. Actually, it may well be that the gas heated by SN explosions is stored in a hot gaseous halo surrounding the satellites, from which it is stripped owing to the interaction with the our Galaxy. In the following, we will only mention galactic winds for the sake of simplicity, but this alternate option (stripping) would work equally well. The gas infall law is the same as in the 2IM or 2IMW models and we only consider a time dependent chemical composition of the infall gas mass.

We take into account the enriched infall from dSph and UfD galaxies predicted by the following 2 models.

(i) Model (i): the infall of gas which forms the Galactic halo is considered primordial up to the time at which the galactic wind in dSphs (or UfDs) starts. After this moment, the infalling gas presents

the chemical abundances of the wind. It is important to underline that for all the Galactic models, the gas infall laws are identical to the reference model presented in Brusadin et al. (2013). As stressed in the previous section, the only thing we are modifying here is the chemical composition of the infalling gas. In figures, we refer to this model with the label 'Name of the reference model+dSph' or 'Name of the reference model+UfD'.

(ii) Model (ii): we explore the case of a diluted infall of gas during the MW halo phase. In particular, after the galactic wind develops in the dSph (or UfD) galaxy, the infalling gas has a chemical composition which, by 50 per cent, is contributed by the dSph (or UfD) outflows; the remaining 50 per cent is contributed by primordial gas of a different extragalactic origin (in agreement with the work of Fiorentino et al. 2015). As stated above, the infall law follows the one assumed in the 2IM or 2IMW models presented in Brusadin et al. (2013). In all the successive figures and in the text, we refer to these models with the labels 'Name of the MW model+dSph (or UfD) MIX'.

In the two upper panels of Fig. 1, we show the evolution in time of the chemical composition of the outflowing gas from the dSph and the UfD galaxy for O, Mg, Si, Ba and Fe. It is worth noting that in the outflows from UfD galaxies, the Fe and Si abundances are larger than in the outflows from dSphs.

We recall that Fe is mostly produced by Type Ia SNe and Si is also produced in a non-negligible amount by the same SNe. Because in our models, the ratio between the time-scale of formation between UfD and dSph is extremely low (τ_{inf}(UfD)/τ_{inf}(dSph) $= 2 \times 10^{-3}$), at later times, the pollution from Type Ia SN is more evident in the UfD outflow. As shown in Tables 2 and 3, in UfDs, the onset of the wind happens at later times compared with dSph objects: t_{gw}(dSph) $< t_{gw}$(UfD).

In the two lower panels the [*X*/Fe] versus [Fe/H] abundance patterns are presented, where *X* corresponds to O, Mg, Si, and Ba.

In Fig. 2 is shown the [O/Fe] ratio as a function of [Fe/H] in the galactic wind of a classical dSph galaxy with characteristics described in Table 2, and compared with the 'MIX' case where the abundances are diluted by 50 per cent by gas of primordial chemical composition. As stated above, in our chemical evolution model for the dSph, the galactic wind begins at 0.013 Gyr after the galaxy formation, and at 0.088 Gyr for the UfD galaxies.
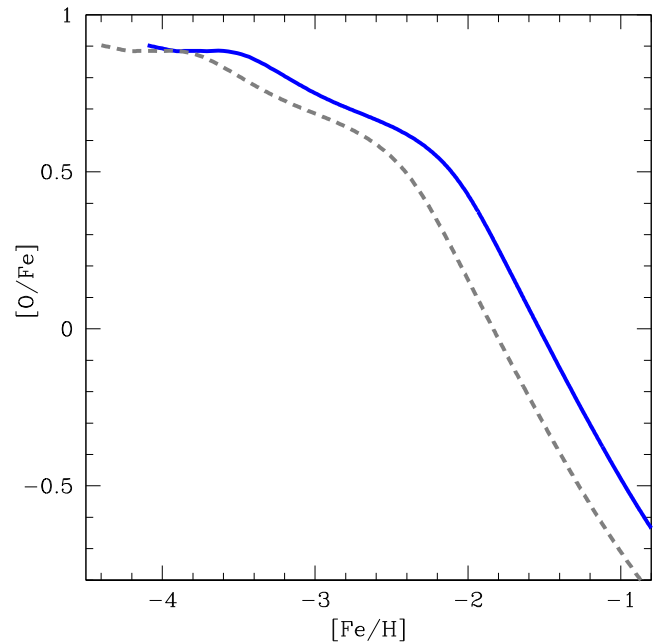
4 THE RESULTS

In this section, we present the results of our chemical evolution models for the Galactic halo, by assuming that either
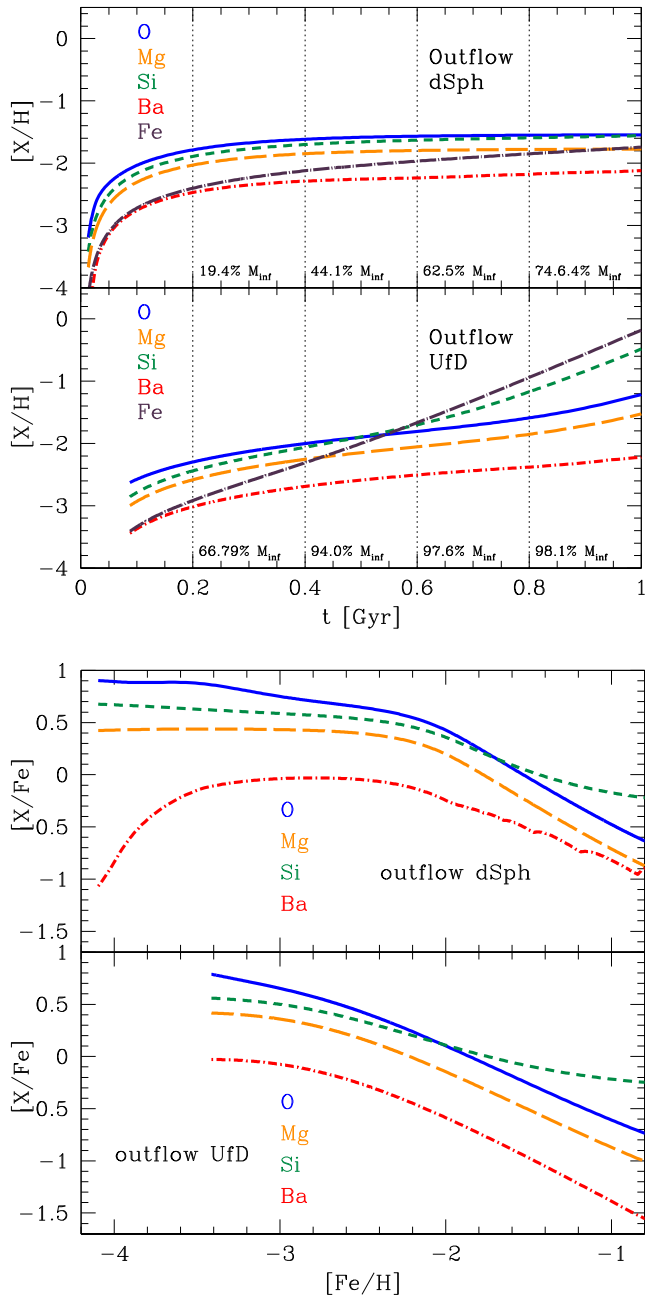
Figure 1. Upper panels: the evolution in time of the chemical abundances for O, Mg, Si, Ba, Fe in the gas ejected as galactic wind from dSphs and UfDs. As shown in Tables 2 and 3, in UfDs, the onset of the wind happens at later times compared with dSph objects: $t_{gw}(dSph) < t_{gw}(UfD)$. We also indicate the cumulative ejected gas mass by outflows at 0.2, 0.4, 0.6, and 0.8 Gyr in terms of percentage of the infall mass M_{inf}. Lower panels: the abundance ratio [X/Fe] as a function of [Fe/H] for the following chemical elements: O, Mg, Si, and Ba of the outflowing gas ejected by a dSph galaxy, and by a UfD galaxy.

(i) all the stars of the Galactic halo were born *in situ* in dSph galaxies

(ii) the Galactic halo formed by accretion of pre-enriched material, originating in dSphs and UfDs (Model i). We explore also the case in which the infalling enriched material is diluted by pristine gas of different extragalactic origin (Model ii).

Figure 2. The abundance ratio [O/Fe] as a function of [Fe/H] of the outflowing gas ejected by the dSph galaxy (blue solid line) compared with the 'mixed' infall model (dashed grey line).

We divide the results in two separate subsections, according to the MW chemical evolution model which is assumed, namely the 2IM (two infall) or the 2IMW (two infall plus outflow) models. It is important to stress out that the models follow the chemical abundances in the ISM and we compare our predictions with stellar abundances under the assumption that their atmospheres reflect the abundances of the ISM out of which they formed.

4.1 The results: the galactic halo in the model 2IM

In Fig. 3, the predicted [O/Fe] versus [Fe/H] abundance patterns are compared with the observed data in Galactic halo stars. In order to directly test the hypothesis that Galactic halo stars have been stripped from dSph or UfD systems, we show the predictions of chemical evolution models for a typical dSph and UfD galaxy (long dashed lines in grey and black, respectively). The two models cannot explain the [α/Fe] plateau which Galactic halo stars exhibit for [Fe/H] ≳ −2.0 dex; in fact, halo stars have always larger [O/Fe] ratios than dSph and UfD stars.

Moreover, in Fig. 3, we show the effects of the enriched infall with chemical abundances taken by the outflowing gas from dSph and Ufd objects on the [O/Fe] versus [Fe/H] relation. In particular, we compare the reference 2IM model for the Galactic halo (which assumes primordial infall) with the '2IM+dSph' and '2IM+UfD' models [enriched infall following Model (i) and (ii) prescriptions, respectively]; in the same figure, we show also the '2IM+ dSph MIX' and '2IM+UfD MIX' models, with chemical abundances of the outflowing gas from dSph and UfD being diluted with primordial ones.

First, we analyse the results with the enriched infall coming from dSph galaxies. We see that, for oxygen, we obtain a better agreement with the data in the halo phase when we consider the enriched infall models. We recall that a key ingredient of the 2IM model is the presence of a threshold in the gas density in the SF fixed at 4 $M_\odot$ pc^{-2} in the halo-thick disc phase. During the halo
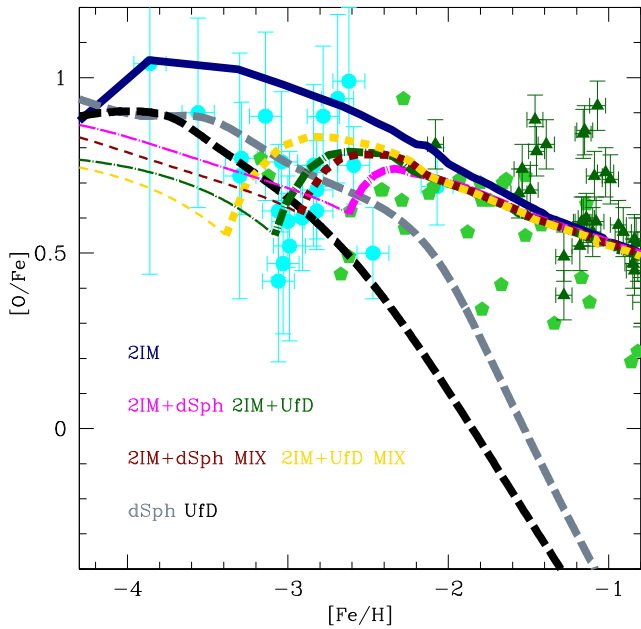
Figure 3. The abundance ratio [O/Fe] as a function of [Fe/H] in the solar neighbourhood for the reference model 2IM is drawn with the solid blue line. Models of the Galactic halo with the enriched infall from dSph: the magenta dash–dotted line and the red short dashed line represent the models 2IM+dSph and 2IM+dSph MIX, respectively. Models of the Galactic halo with the enriched infall from UfDs: the green dash–dotted line and the yellow short dashed line represent the models 2IM+UfD and 2IM+UfD MIX, respectively. Thinner lines indicate the ISM chemical evolution phases in which the SFR did not start yet in the Galactic halo, and during which stars are no created. Models of the dSph and UfD galaxies: the long dashed grey line represents the abundance ratios for the dSph galaxies, whereas long dashed black line for the UfD galaxies. Observational data of the Galactic halo: Cayrel et al. (2004) (cyan circles), Akerman et al. (2004) (light green pentagons), Gratton et al. (2003) (dark green triangles).

phase, such a critical threshold is reached only at $t = 0.356$ Gyr from the Galaxy formation. On the other hand, when including the environmental effect, we have to consider also the time for the onset of the galactic wind, which in the dSph model occurs at $t_{gw} = 0.013$ Gyr.

Therefore, the SF begins after 0.356 Gyr from the beginning of Galaxy formation, and this fact explains the behaviour of the curves with enriched infalls in Fig. 3: during the first 0.356 Gyr in both '2IM+dSph' and '2IM+dSph MIX' models, no stars are created, and the chemical evolution is traced by the exponential gas accretion with a time-dependent chemical enrichment (equation 3).

In Fig. 3 and in all the successive figures, we indicate with thinner lines the ISM chemical evolution phases in which the SFR did not start yet in the Galactic halo, and during which stars are no created.

To summarize, for the model '2IM+dSph' we distinguish three different phases in the halo chemical evolution.

(i) Phase (1): 0–0.013 Gyr, the infall is primordial, the wind in dSphs has not started yet, and there is no SF;

(ii) Phase (2): 0.013–0.356 Gyr, the infall is enriched by dSphs, the SFR is zero in this phase;

(iii) Phase (3): 0.356–1 Gyr; the infall is enriched by dSphs, the SFR is different from zero.

During phase (3), the SF takes over, and increases the [O/Fe] values because of the pollution from massive stars on short time-scales.
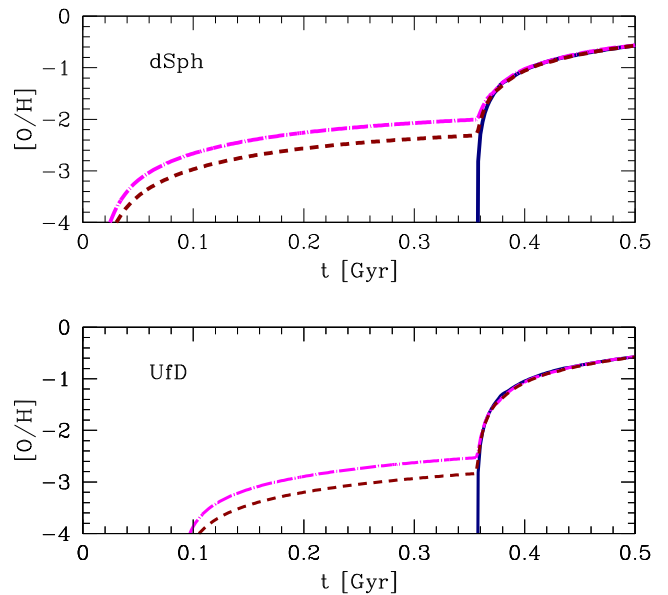
Figure 4. Upper panel: the abundance ratio [O/H] as a function of Galactic time in the solar neighbourhood. We compared the 2IM model (blue solid line) with the model where we have taken into account the enriched infall from dSph galaxies (model 2IM+dSph with dash–dotted magenta line). With the short dashed red line, we represent the model 2IM+dSph MIX. Lower panel: As in the upper panel but considering the enriched gas from UfD galaxies.

We note that the entire spread of the data cannot be explained assuming a time-dependent enriched infall with the same abundances of the outflowing gas from dSph galaxies, even if there is a better agreement with the halo data in comparison to the model with primordial infall.

It is important to underline that, until the SF is non-zero, no stars are created; however, since our models follow the chemical abundances in the gas phase, the solely contribution to the ISM chemical evolution before SF begins is due to the time dependent enriched infall. It means that in the '2IM+dSph' model, the first stars that are formed have [Fe/H] values larger than −2.4 dex.

In this case, to explain data for stars with [Fe/H] smaller than −2.4 dex, we need stars formed in dSph systems (see the model curve of the chemical evolution of dSph galaxies).

Concerning the results with the enriched infall from UfD outflow abundances, we recall here that in our reference model for UfD galaxies, the wind starts at 0.08 Gyr. The model results for the halo still reproduce the data but with the same above mentioned caveat.

In Fig. 4, we show the time evolution of oxygen abundances for the model 2IM (primordial infall), 2IM+dSph, 2IM+dSph MIX, 2IM+UfD, and 2IM+UfD MIX. We notice that the reference model 2IM, as explained before, shows chemical evolution after $t = 0.356$ Gyr, and the models with enriched infalls which show the fastest chemical enrichment are the ones with infall abundances taken from the outflows of dSph objects, because the galactic winds occur earlier than in UfD systems.

In Figs 5 and 6, we show the results of all our chemical evolution models with the 2IM scenario for the [Si/Fe] and [Mg/Fe] versus [Fe/H] abundance patterns, respectively. The various curves with different colours represent the same chemical evolution models as in Fig. 3. As concluded for the [O/Fe] versus [Fe/H] abundance diagram, our reference chemical evolution models for dSph and UfD galaxies cannot explain the observed Galactic halo data over
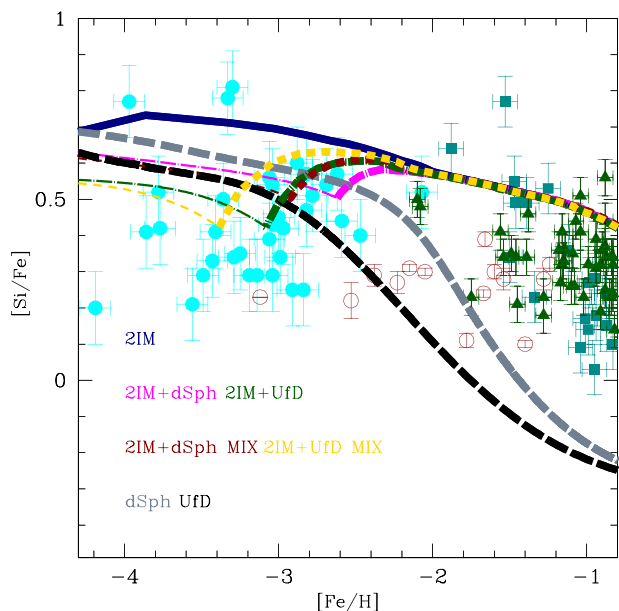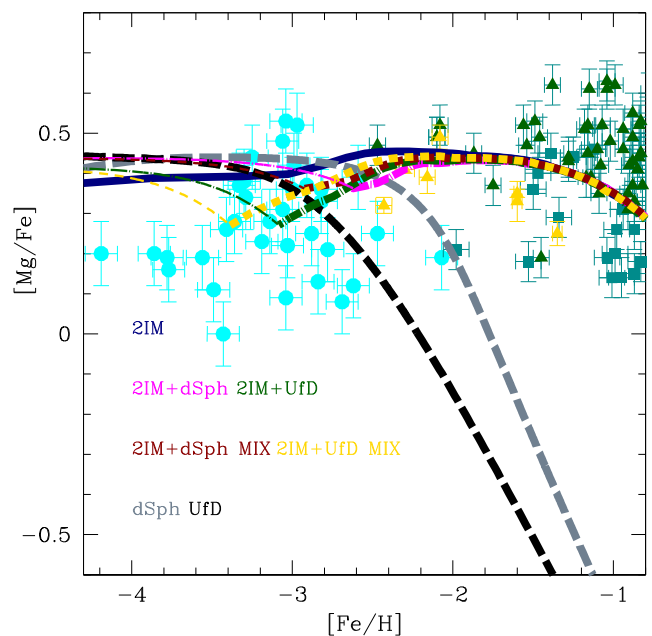
Figure 5. The abundance ratio [Si/Fe] as a function of [Fe/H] in the solar neighbourhood. Models of the Galactic halo with the enriched infall from dSph: the magenta dash–dotted line and the red short dashed line represent the models 2IM+dSph and 2IM+dSph MIX, respectively. Models of the Galactic halo with the enriched infall from UfDs: the green dash–dotted line and the yellow short dashed line represent the models 2IM+UfD and 2IM+UfD MIX, respectively. Models of the dSph and UfD galaxies: the long dashed grey line represents the abundance ratios for the dSph galaxies, whereas long dashed black line for the UfD galaxies. Observational data of the Galactic halo: Cayrel et al. (2004) (cyan circles), Shi et al. (2009) (open brown circles), Reddy, Lambert & Allende Prieto (2006) (filled blues squares), Gratton et al. (2003) (dark green triangles).
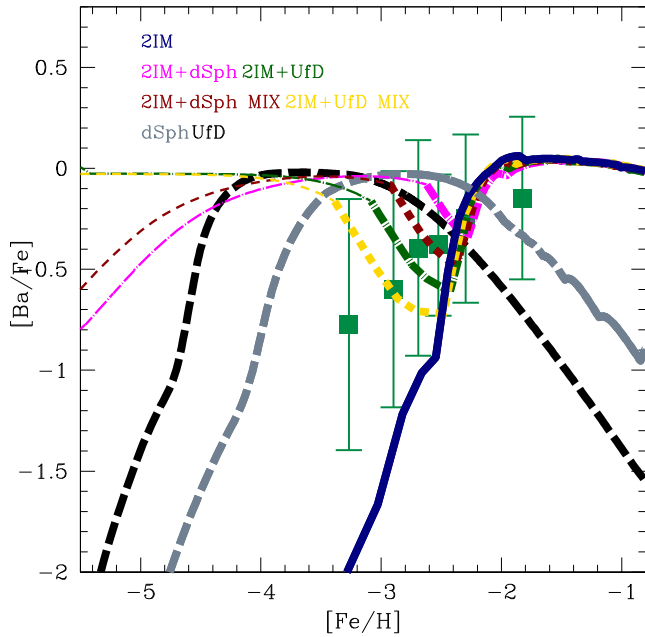

Figure 6. The abundance ratio [Mg/Fe] as a function of [Fe/H] in the solar neighbourhood. Models of the Galactic halo with the enriched infall from dSph: the magenta dash–dotted line and the red short dashed line represent the models 2IM+dSph and 2IM+dSph MIX, respectively. Models of the Galactic halo with the enriched infall from UfDs: the green dash–dotted line and the yellow short dashed line represent the models 2IM+UfD and 2IM+UfD MIX, respectively. Models of the dSph and UfD galaxies: the long dashed grey line represents the abundance ratios for the dSph galaxies, whereas long dashed black line for the UfD galaxies. Observational data of the Galactic halo: Cayrel et al. (2004) (cyan circles), Mashonkina et al. (2007) (yellow triangles), Reddy et al. (2006) (filled blues squares), Gratton et al. (2003) (dark green triangles).

the entire range of [Fe/H] abundances. This rules out the hypothesis that all Galactic halo stars were stripped or accreted in the past from dSphs or UfDs. This result is in agreement with previous works in the literature as the ones of Unavane at al. (1996) and Venn et al. (2004). On the other hand, as stated above, if we assume that the Galactic halo formed by accreting enriched gas from dSphs or UfDs, we also need a stellar contribution from dSphs and UfDs to explain the stars at very low [Fe/H] that currently reside in the halo.

It is worth noting that for the α elements studied in this work, all models predictions including the enriched infall of gas, tend to the [α/Fe] values of the reference model for high [Fe/H] in the halo phase. This is due to the fact that when the SF is active, the pollution from dying stars overcomes the enriched infall effects.

We note that a different value of the threshold in the MW model would modify the duration of the phase (2). In this work, we did not explore different values of the threshold in the halo, our aim being to test the effects of the enriched infall on chemical evolution models of the MW, which are able to reproduce the majority of the observations in the solar neighbourhood and also the abundance gradients along the disc. As shown in Mott, Spitoni & Matteucci (2013), if we do not take into account radial gas flows (Portinari & Chiosi 2000; Spitoni & Matteucci 2011; Cavichia et al. 2014), a threshold in the gas density is required to explain the abundance gradients along the Galactic disc, and in particular the values of $4 \, M_\odot \, pc^{-2}$ in the halo phase and $7 \, M_\odot \, pc^{-2}$ in the thin disc phase, provide a very good agreement with the data.

In Fig. 7, we show the results for the [Ba/Fe] versus [Fe/H] abundance diagram. The observational data are from Frebel (2010),

as selected and binned by Cescutti et al. (2013). By looking at the figure, the 2IM model does not provide a good agreement with the observed data set for [Fe/H] < −2.5 dex. The initial increasing trend of the [Ba/Fe] ratios in the 2IM model is due to the contribution of the first Ba-producers, which are massive stars with mass in the range 12–30 $M_\odot$.

By looking at Fig. 7, one can also appreciate that our chemical evolution models for dSphs and UfDs fail in reproducing the observed data, since they predict the [Ba/Fe] ratios to increase at much lower [Fe/H] abundances than the observed data. Concerning the chemical evolution of the Ba for dSphs, our predictions are in agreement with Lanfranchi, Matteucci & Cescutti (2008), where they compared the evolution of *s*- and *r*- process elements in our Galaxy with that in dSph galaxies. That is due to the very low SFEs assumed for dSphs and UfDs, which cause the first Ba-polluters to enrich the ISM at extremely low [Fe/H] abundances. The subsequent decrease of the [Ba/Fe] ratios is due to the large iron content deposited by Type Ia SNe in the ISM, which happens at still very low [Fe/H] abundances in dSphs and UfDs. Hence, in the range $-3.5 \lesssim$ [Fe/H] $\lesssim -2.5$ dex, while Galactic halo stars exhibit an increasing trend of the [Ba/Fe] versus [Fe/H] abundance ratio pattern, UfD stars show a decreasing trend (see also Koch et al. 2013).

In Fig. 7, all our models involving an enriched infall from dSphs and UfDs deviate substantially from the observed trend of the [Ba/Fe] versus [Fe/H] abundance pattern in Galactic halo stars.

Figure 7. The abundance ratio [Ba/Fe] as a function of [Fe/H] in the solar neighbourhood. Models of the Galactic halo with the enriched infall from dSph: the magenta dash–dotted line and the red short dashed line represent the models 2IM+dSph and 2IM+dSph MIX, respectively. Models of the Galactic halo with the enriched infall from UfDs: the green dash–dotted line and the yellow short dashed line represent the models 2IM+UfD and 2IM+UfD MIX, respectively. Models of the dSph and UfD galaxies: the long dashed grey line represents the abundance ratios for the dSph galaxies, whereas long dashed black line for the UfD galaxies. Observational data of the Galactic halo: Frebel (2010).

Such a discrepancy enlarges for [Fe/H] < −2.4 dex, where those models predict always larger [Ba/Fe] ratios than the 2IM model.

4.2 The results: the galactic halo in the model 2IMW

In this subsection, we show the results when the time dependent enriched infall is applied to the reference model 2IMW. In Fig. 8, we show the results in terms of [O/Fe] versus [Fe/H] in the solar neighbourhood.

As mentioned in Section 2, the reference model 2IMW in the halo phase is characterized by an outflow gas rate proportional to the SFR and by a smaller formation time-scale τ_H than the one of the model 2IM (see Table 1). A shorter formation time-scale leads to a faster chemical evolution at the early times. In fact, as shown in fig. 2 of Brusadin et al. (2013), the SFR starts at 0.05 Gyr, since the critical threshold in the surface gas density is reached earlier.

As done above, for the model '2IMW+dSph', we distinguish three different phases in the halo chemical evolution.

(i) Phase (1): 0–0.013 Gyr, the infall is primordial, the wind in dSphs has not started yet and there is no SF;

(ii) Phase (2): 0.013–0.05 Gyr, the infall is enriched by dSphs, the SFR is zero in this phase;

(iii) Phase 3): 0.05–1 Gyr; the infall is enriched by dSphs, the SFR is different from zero.

On one hand, comparing model '2IMW+dSph' in Fig. 8 with model '2IM+dSph' in Fig. 3, we can see that the former shows a shorter phase (2) than the latter.
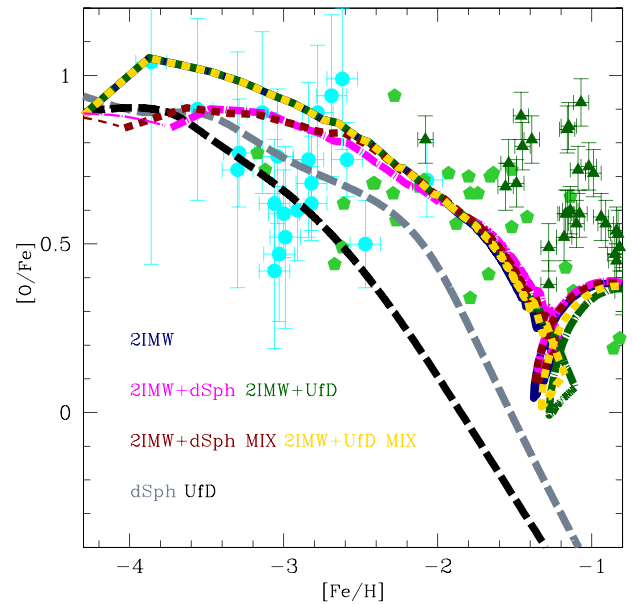
Figure 8. The abundance ratio [O/Fe] as a function of [Fe/H] in the solar neighbourhood as in Fig. 3 but for the 2IMW model.

On the other hand, comparing model '2IMW+UfD' in Fig. 8 with model '2IM+UfD' in Fig. 3, we see that the former overlap to the reference model 2IMW at almost all [Fe/H] abundances. In fact, since in the UfD galactic model the wind starts at 0.088 Gyr and, at this instant, in the model 2IMW the SF is already active (the SF activity begins at 0.05 Gyr), the phase (2) evolution (namely, chemical evolution without SF) is not present in the 2IMW+UfD model. Therefore, the effect of the enriched infall is almost negligible compared to the pollution of chemical elements produced by dying halo stars, since we cannot distinguish between the effect of an enriched infall from UfDs and the chemical feedback provided by the Type II SNe originated in the Galactic halo itself.

This can also be appreciated by looking at Fig. 9, where the time evolution of the oxygen abundances of the model 2IMW, and in presence of enriched infall from UfD and dSph galaxies are shown. We see that for the UfD case the model with enriched infall is almost identical to the reference model 2IMW.

In Figs 10 and 11, model results for [Si/Fe] versus [Fe/H] and [Mg/Fe] versus[Fe/H] in the solar neighbourhood are presented, respectively. As for oxygen, the effect of the enriched infall from UfD galaxies is almost negligible compared to the pollution of chemical elements produced by dying halo stars.

Concerning the [Ba/Fe] versus [Fe/H] abundance pattern, in Fig. 12, we compare the predictions of our models with the Galactic halo data. We notice that the 2IMW model provides now a better agreement with the observed data than the 2IM model, although the predicted [Ba/Fe] ratios at [Fe/H] < −3 dex still lie below the observed data. On the other hand, by assuming an enriched infall from dSph or UfD galaxies, the predicted [Ba/Fe] ratios agree with the observed data also at [Fe/H] < −3 dex. In conclusion, in order to reproduce the observed [Ba/Fe] ratios over the entire range of [Fe/H] abundances, a time-dependent enriched infall in the Galactic halo phase is required. We are aware that for Ba more detailed data are needed, therefore at this stage, we cannot draw firm conclusions.

We note that in general [α/Fe] ratios in dSphs and UfDs can overlap with those of halo stars at very low metallicity, where in all
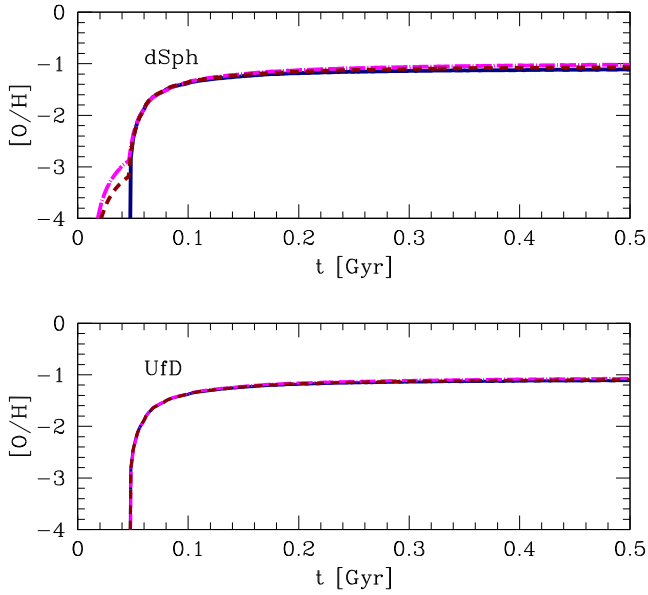
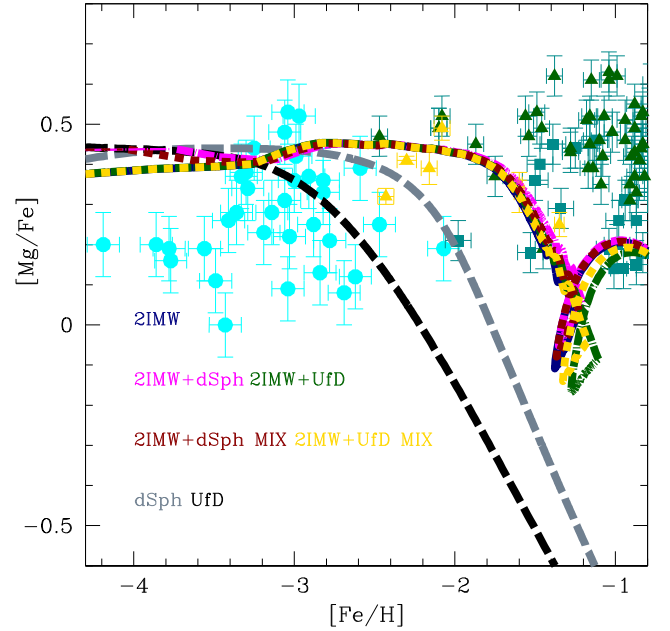**Figure 9.** As in Fig. 4, the evolution in time for oxygen but for the 2IMW model.
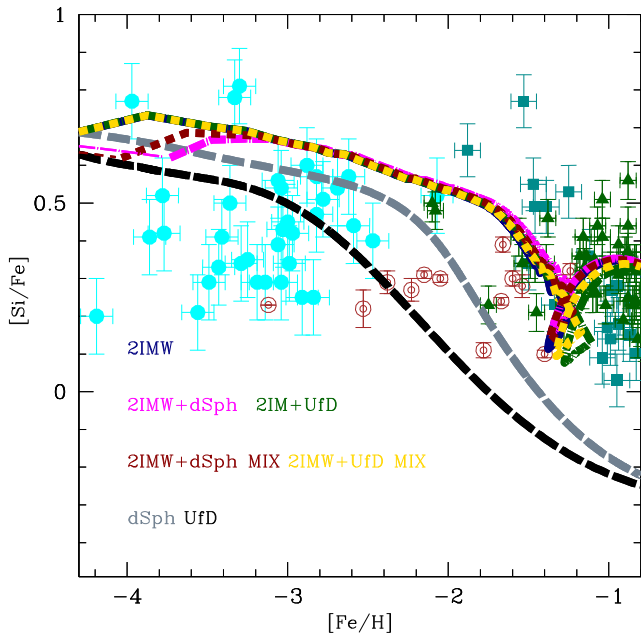
Figure 10. The abundance ratio [Si/Fe] as a function of [Fe/H] in the solar neighbourhood. As in Fig. 5 but for the 2IMW model.
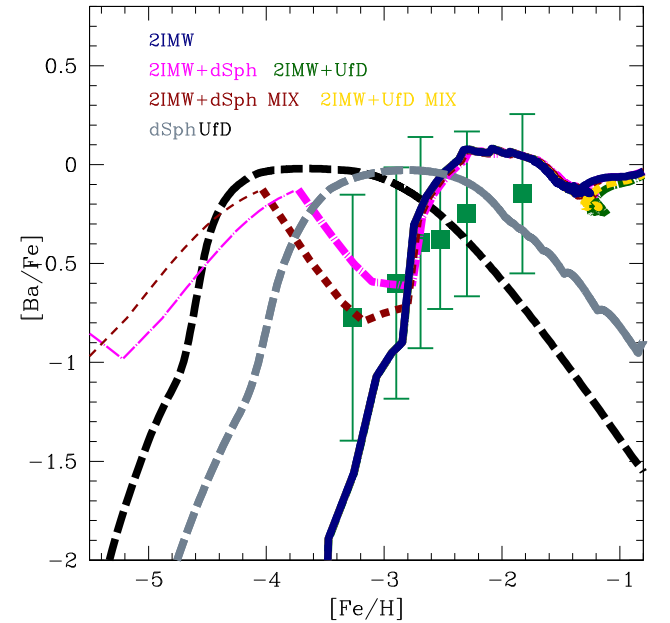
Figure 11. The abundance ratio [Mg/Fe] as a function of [Fe/H] in the solar neighbourhood. As in Fig. 6 but for the 2IMW model.

Figure 12. The abundance ratio [Ba/Fe] as a function of [Fe/H] in the solar neighbourhood. As in Fig. 7 but for the 2IMW model.

galaxies, the chemical enrichment is dominated by the nucleosynthesis of core collapse SNe.

This makes difficult to test whether some stars from dwarf satellites have indeed been accreted by the halo. Rather, it is likely that a fraction as high as 50 per cent of the gas out of which the halo formed has been shed by its satellite systems, whose relics we see (in part) nowadays, devoid of their gas. This is only valid for satellite systems with a very short duration of SF, as modelled in this paper. More realistic SFH would create ejected gas with low [α/Fe] (as seen in the stars in the surviving luminous dSph) and conflict with the data for halo stars.

On the other hand, we have identified in the [Ba/Fe] ratios a better discriminant of the origin of halo stars. The differences predicted

for the dwarf galaxies relative to the halo suggest that it is unlikely that the dSphs and UfDs have been the building blocks of the halo.

In Fig. 13, we show the predicted G-dwarf distributions in terms of [Fe/H] for models of Figs 3 and 8. Our predictions have been convolved with a Gaussian with an error of 0.2 dex. As pointed out by Brusadin et al. (2013), the reference model 2IM is not able to reproduce the peak of the distribution. Only assuming a shorter formation time-scale coupled with a gas outflow event in the Galactic halo chemical evolution (model 2IMW) we are able to properly fit the observed distribution. Anyway, in both cases, the enriched infall of gas from dSph and UfD objects does not affect the distributions. In Fig. 14, the G-dwarf distribution is shown as a
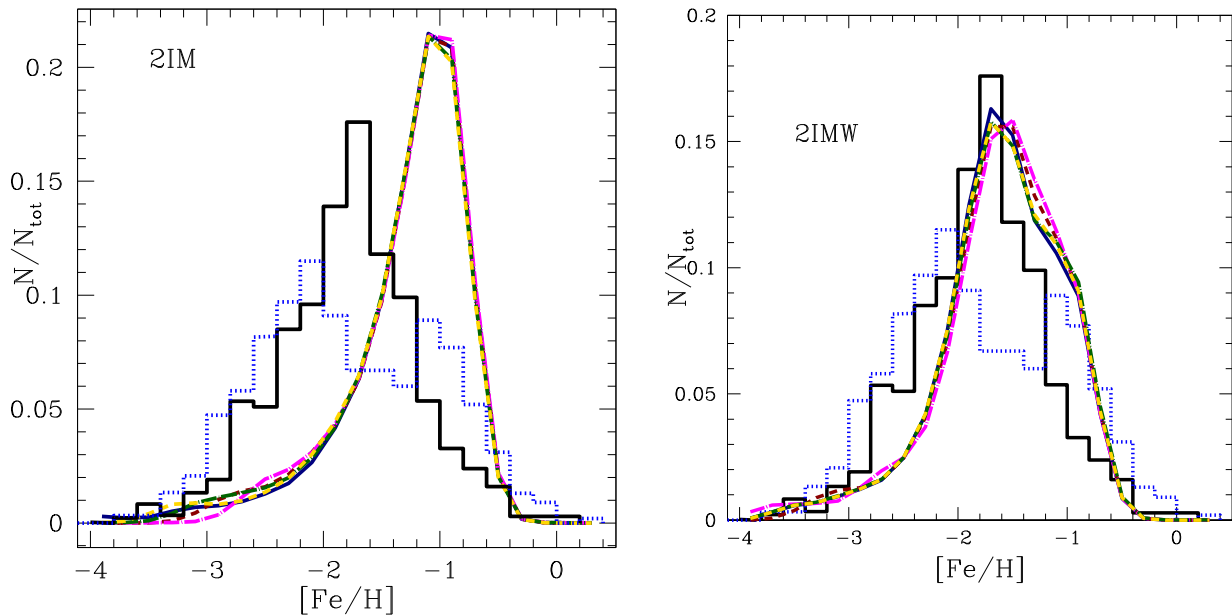
Figure 13. The G-dwarf metallicity distributions ([Fe/H]) predicted by models with enriched infall of gas based on the reference 2IM model (left-hand panel) and the ones based on the 2IMW model (right-hand panel), are compared to the observed distributions by Ryan & Norris (1991, dotted blue histogram) and Schörck et al. (2009, solid black histogram). Concerning the left-hand panel, model colour lines are the same as in Fig. 3, on the other hand in the right-hand panel, colour lines are the same as in Fig. 8. Our predictions have been convolved with a Gaussian with an error of 0.2 dex.
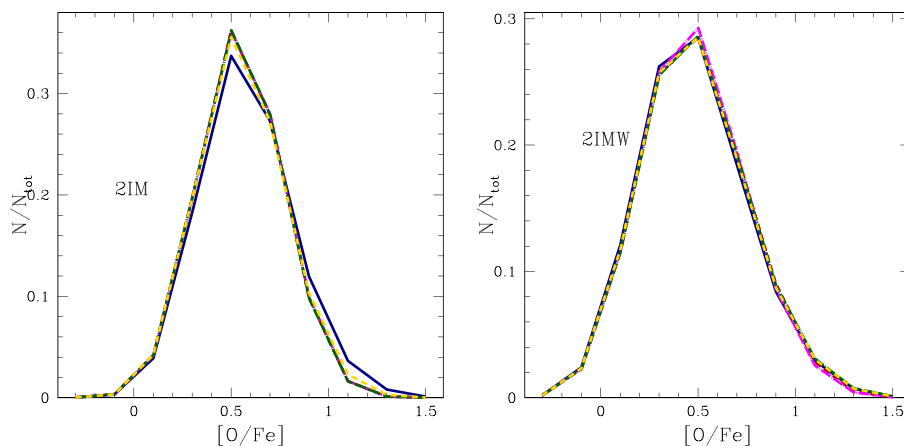
Figure 14. The G-dwarf distributions in terms of [O/Fe] predicted by models with enriched infall of gas based on the reference 2IM model (left-hand panel) and the ones based on the 2IMW model (right-hand panel). Concerning the left-hand panel, model colour lines are the same as in Fig. 3, on the other hand in the right-hand panel, colour lines are the same as in Fig. 8. Our predictions have been convolved with a Gaussian with an error of 0.2 dex.

function of the [O/Fe] ratio. Here, both models 2IM and 2IMW, including the enriched infall models show the peak at 0.5 dex.

5 CONCLUSIONS

In this paper, we first have explored the hypothesis that dSph and UfD galaxies are the survived building blocks of the Galactic halo, by assuming that the halo formed by accretion of stars belonging to these galaxies.

Then, we have presented a different scenario in which the Galactic halo formed by accretion of enriched gas with the same chemical composition as the outflowing gas from dSphs and UfDs. Finally, we have tested the effect of diluting the infalling material from dSphs or UfDs with primordial gas of different extragalactic origin.

Our main conclusions can be summarized as follows.

(i) We find that the predicted [α/Fe] versus [Fe/H] abundance patterns of UfD and dSph chemical evolution models deviate substantially from the observed data of the Galactic halo stars only for [Fe/H] values larger than −2 dex; this means that at those metallicities, the chemical evolution of the Galactic halo was different than in the satellite galaxies. On the other hand, we notice that for Ba, the chemical evolution models of dSphs and UfDs fail to reproduce the observational observed data of the Galactic halo stars over the whole range of [Fe/H].

(ii) We can safely rule out the hypothesis that the stellar halo of the MW entirely formed from the merging of galaxies which were the ancestors of the current dSphs and UfDs. Our results are in agreement with the previous suggestions of Unavane et al. (1996) and Venn et al. (2004). We cannot rule out, however, the hypothesis

that a substantial contribution to the formation of the Galaxy stellar halo was provided by a population of dwarf galaxies which were more massive and more evolved from the point of view of the ISM chemical evolution than the current dSphs and UfDs.

(iii) Concerning the chemical evolution models for the MW in the presence of enriched gas infall, we obtain that: the effects on the [α/Fe] versus [Fe/H] plots depend on the infall time-scale for the formation of the halo and the presence of a gas threshold in the SF. In fact, the most evident effects are present for the model 2IM, characterized by the longest time-scale of formation (0.8 Gyr), and the longest period without SF activity among all models presented here.

(iv) In general, the enriched infall by itself is not capable to explain the observational spread in the halo data at low [Fe/H], in the [α/Fe] versus [Fe/H] plots. Moreover, in the presence of an enriched infall, we need stars produced *in situ* in dSph or UfD objects and accreted later to the Galactic halo, to explain the data at lowest [Fe/H] values.

(v) The optimal element to test different theories of halo formation is barium which is (relatively) easily measured in low-metallicity stars. In fact, we have shown that the predicted [Ba/Fe] versus [Fe/H] relation in dSphs and UfDs is quite different than in the Galactic halo. Moreover, the [Ba/Fe] ratio can be substantially influenced by the assumption of an enriched infall. In particular, the two infall plus outflow model can better reproduce the data in the whole range of [Fe/H] abundances, and this is especially true if a time-dependent enriched infall during the halo phase is assumed.

ACKNOWLEDGEMENTS

REFERENCES

Akerman C. J., Carigi L., Nissen P. E., Pettini M., Asplund M., 2004, A&A, 414, 93
Belokurov V. et al., 2006a, ApJ, 642, L137
Belokurov V. et al., 2006b, ApJ, 647, L111
Belokurov V. et al., 2007, ApJ, 654, 897
Brown T. M. et al., 2012, ApJ, 753, L21
Brusadin G., Matteucci F., Romano D., 2013, A&A, 554, A135
Bullock J. S., 2010, preprint (arXiv:1009.4505)
Busso M., Gallino R., Lambert D. L., Travaglio C., Smith V. V., 2001, ApJ, 557, 802
Cavichia O., Molla M., Costa R. D. D., Maciel W. J., 2014, MNRAS, 437, 3688
Cayrel R. et al., 2004, A&A, 416, 1117
Cescutti G., François P., Matteucci F., Cayrel R., Spite M., 2006, A&A, 448, 557
Cescutti G., Chiappini C., Hirschi R., Meynet G., Frischknecht U., 2013, A&A, 553, A51
Chiappini C., Matteucci F., Gratton R., 1997, ApJ, 477, 765
Chiappini C., Matteucci F., Romano D., 2001, ApJ, 554, 1044
Ekström S., Meynet G., Chiappini C., Hirschi R., Maeder A., 2008, A&A, 489, 685
Fiorentino G. et al., 2015, ApJ, 798, L12
Font A. S., Johnston K. V., Bullock J. S., Robertson B. E., 2006, ApJ, 638, 585
François P., Matteucci F., Cayrel R., Spite M., Spite F., Chiappini C., 2004, A&A, 421, 613
Frebel A., 2010, Astron. Nachr., 331, 474
Freeman K. C., 2010, in Block D. L., Freeman K. C., Puerari I., eds, Galaxies and their Masks, p. 319
Gilmore G. et al., 2012, The Messenger, 147, 25
Gratton R. G., Carretta E., Desidera S., Lucatello S., Mazzei P., Barbieri M., 2003, A&A, 406, 131
Grebel E. K., 2005, in Jerjen H., Binggeli B., eds, IAU Colloq. 198: Near-fields Cosmology with Dwarf Elliptical Galaxies. Cambridge Univ. Press, Cambridge, p. 1
Hartwick F., 1976, ApJ, 209, 418
Hirschi R., 2005, in Hill V., François P., Primas F., eds, Proc. IAU Symp. 228, From Lithium to Uranium: Elemental Tracers of Early Cosmic Evolution. Kluwer, Dordrecht, p. 331
Hirschi R., 2007, A&A, 461, 571
Iwamoto K., Brachwitz F., Nomoto K., Kishimoto N., Umeda. H., Hix W. R., Thielemann F. K., 1999, ApJS, 125, 439
Jofré P., Weiss A., 2011, A&A, 533, A59
Karakas A. I., 2010, MNRAS, 403, 1413
Kennicutt R. C., Jr, 1998, ApJ, 498, 541
Klypin A., Gottlöber S., Kravtsov A. V., Khokhlov A. M., 1999, ApJ, 516, 530
Kobayashi C., Umeda H., Nomoto K., Tominaga N., Ohkubo T., 2006, ApJ, 653, 1145
Koch A., Feltzing S., Adén D., Matteucci F., 2013, A&A, 554, A5
Kuijken K., Gilmore G., 1991, ApJ, 367, L9
Lanfranchi G. A., Matteucci F., Cescutti G., 2008, A&A, 481, 635
Majewski S. R., Wilson J. C., Hearty F., Schiavon R. R., Skrutskie M. F., 2010, in Cunha K., Spite M., Barbuy B., eds, Proc. IAU Symp. 265, Chemical Abundances in the Universe: Connecting First Stars to Planets. Kluwer, Dordrecht, p. 480
Mashonkina L., Korn A. J., Przybilla N., 2007, A&A, 461, 261
Matteucci F., 2001, The Chemical Evolution Of The Galaxy. Kluwer Academic Publishers, Dordrecht
Matteucci F., François P., 1989, MNRAS, 239, 885
Meynet G., Maeder A., 2002, A&A, 390, 561
Micali A., Matteucci F., Romano D., 2013, MNRAS, 436, 1648
Moore B., Ghigna S., Governato F., Lake G., Quinn T., Stadel J., Tozzi P., 1999, ApJ, 524, L19
Mott A., Spitoni E., Matteucci F., 2013, MNRAS, 435, 2918
Norris J. E., Gilmore G., Wyse R. F. G., Wilkinson M. I., Belokurov V., Evans N. W., Zucker D. B., 2008, ApJ, 689, L113
Norris J. E., Yong D., Frebel A., Wilkinson M. I., Belokurov V., Zucker D. B., 2010, ApJ, 723, 1632
Portinari L., Chiosi C., 2000, A&A, 355, 929
Prantzos N., 2008, A&A, 489, 525
Press W. H., Schechter P., 1974, ApJ, 187, 425
Recchi S., Spitoni E., Matteucci F., Lanfranchi G. A., 2008, A&A, 489, 555
Reddy B. E., Lambert D. L., Allende Prieto C., 2006, MNRAS, 367, 1329
Romano D., Karakas A. I., Tosi M., Matteucci F., 2010, A&A, 522, A32
Romano D., Bellazzini M., Starkenburg E., Leaman R., 2015, MNRAS, 446, 4220
Ryan S., Norris J., 1991, AJ, 101, 1865
Salpeter E. E., 1955, ApJ, 121, 161
Scalo J. M., 1986, Fundam. Cosm. Phys., 11, 1
Schmidt M., 1959, ApJ, 129, 243
Schörck T. et al., 2009, A&A, 507, 817
Shetrone M. D., Côté P., Sargent W. L. W., 2001, ApJ, 548, 592
Shi J. R., Gehren T., Mashonkina L., Zhao G., 2009, A&A, 503, 533
Spitoni E., 2015, MNRAS, 451, 1090
Spitoni E., Matteucci F., 2011, A&A, 531, A72
Spitoni E., Calura F., Matteucci F., Recchi S., 2010, A&A, 514, A73
Springel V., Frenk C. S., White S. D. M., 2006, Nature, 440, 1137
Steinmetz M. et al., 2006, AJ, 132, 1645
Tollerud E. J., Bullock J. S., Strigari L. E., Willman B., 2008, ApJ, 688, 277
Unavane M., Wyse R. F. G., Gilmore G., 1996, MNRAS, 278, 727

Venn K. A., Irwin M., Shetrone M. D., Tout C. A., Hill V., Tolstoy E., 2004, AJ, 128, 1177

Vincenzo F., Matteucci F., Vattakunnel S., Lanfranchi G. A., 2014, MNRAS, 441, 2815

Weisz D. R., Johnson B. D., Conroy C., 2014, ApJ, 794, L3

White S. D. M., Rees M. J., 1978, MNRAS, 183, 341

White S. D. M., Springel V., 2000, in Weiss A., Abel T. G., Hill V., The First Stars. Springer-Verlag, Berlin, p. 327

Willman B. et al., 2005, AJ, 129, 2692

Woosley S. E., Weaver T. A., 1995, ApJS, 101, 181

Yanny B. et al., 2009, AJ, 137, 4377

York D. G. et al., 2000, AJ, 120, 1579

This paper has been typeset from a TEX/LATEX file prepared by the author.